Non-invasive brain perfusion MRI using endogenous deoxyhemoglobin as a contrast agent: preliminary data

J. Poublanc[1], O. Sobczyk[1,7], R. Shafi[1], J. Duffin[3,7], K. Uludag[4,8], J. Wood[5], C. Vu[6], R. Dharmakumar[6], J.A. Fisher[3,7], *D.J. Mikulis[1,2,4]

*Correspondence to david.mikulis@uhn.ca

1. Joint Department of Medical Imaging and the Functional Neuroimaging Lab, University Health Network, Toronto, ON, Canada

2. The Joint Department of Medical Imaging, The Toronto Western Hospital, The University of Toronto

3. Department of Physiology, University of Toronto, Toronto, Ontario, Canada.

4. Techna Institute & Koerner Scientist in MR Imaging, University Health Network, Toronto, Canada

5. Division of Cardiology, Department of Pediatrics and Radiology, Children's Hospital Los Angeles, Los Angeles, CA.

6. Department of Biomedical Engineering, University of Southern California, Los Angeles, CA.

7. Department of Anaesthesia and Pain Management, University Health Network, University of Toronto, Toronto, ON, Canada.

8 Center for Neuroscience Imaging Research, Institute for Basic Science & Department of Biomedical Engineering, Sungkyunkwan University, Suwon, Republic of Korea

Abstract

Background: The paramagnetic properties of deoxyhemoglobin shorten T2* as do gadolinium based contrast agents. Induction of abrupt changes in arterial deoxyhemoglobin concentration ([dOHb]) can mimic the action of intra-vascular boluses of gadolinium based contrast agents (GBCAs) used for perfusion imaging.

Aim: To demonstrate the feasibility of rapidly changing pulmonary venous hemoglobin saturation for generating boluses of blood with altered T2* properties for measuring flow metrics in the systemic circulation.

Methods: A gas blender with a sequential gas delivery breathing circuit and software enabling prospective arterial blood gas targeting was used to implement rapid lung changes in the partial pressure of blood oxygen (PaO_2) while maintaining isocapnea. Lung PaO_2 was initially lowered to induce a low baseline deoxyhemoglobin concentration [dOHb]. PaO_2 was then rapidly raised to normal for 10 seconds and then rapidly lowered to the initial low baseline creating a oxyhemoglobin (OHb) bolus. R2* changes were measured using blood oxygenation dependent (BOLD) MRI signal changes in large arteries and veins as well as in the microcirculation. This enabled generation of the following maps: bolus arrival time delay (TD) cerebral blood volume (CBV), mean transit time (MTT) and cerebral blood flow (CBF). **Results:** BOLD signal in the middle cerebral artery showed a sharp increase during the OHb bolus transit indicating minimal dispersion confirming effective rapid modulation of pulmonary venous PO_2 with reasonable cortical contrast-to-noise ratio of 3. Signals sorted by amplitude of signal changes and arrival times enabled the visualization of major arteries and veins.

Contrast to noise ratio was adequate for a single gas challenge to provide most of the contrast, little improved by averaging over the remaining set of challenges. Values of the flow metrics derived from the perfusion maps were within normal ranges from published literature values.

Conclusion: Non-invasive induction of abrupt changes in OHb saturation can function as a novel non-invasive vascular contrast agent for use in perfusion imaging.

MANUSCRIPT

Introduction

Blood-Oxygenation-Level-Dependent (BOLD) sequences are sensitive to distortions in the static magnetic field caused by paramagnetic agents such as deoxyhemoglobin and gadolinium based contrast agents (GBCAs)[1]**.** When arterial blood arrives fully oxygenated at the tissues, the balance between tissue oxygen consumption and blood flow determine the capillary and venous deoxyhemoglobin concentration ([dOHb]) and thus the BOLD signal. The BOLD signal follows an exponential decay with a time constant T2*. There are near linear > 3-fold increases in intra-vascular T2* with decreasing hemoglobin (Hb) O_2 saturation to 50% [2 3]. The effect is also relatively linear at a field strength of 3T [4] and is an order of magnitude greater than that associated with signal changes seen in the tissue [5]. The considerable change in intra-vascular T2* signal related to [dOHb] has the potential to act as an endogenous MRI contrast agent. In order to focus on changes in [dOHb], we restricted the PO_2 range from ~100 mmHg

(normoxia) to about ~30 mmHg, corresponding to 50% desaturation[6]. Specifically, the range of interest excludes all hyperoxic levels > 100 mmHg, at which at which there is little or no arterial [dOHb].

The generation of dOHb as a contrast agent has not previously been exploited for hemodynamic studies due to the difficulty in generating a series of inspired PO_2 and PCO_2 concentrations calculated to attain and maintain targeted transient abrupt changes in lung PO_2 while maintaining normocapnia (resting arterial PCO_2). Once solved, the remaining physiology is conducive to generating abrupt changes in pulmonary venous dOHb for distribution to the systemic circulation via the left heart with little subsequent dispersion. The lungs are exceptionally effective at generating Hb boluses with altered blood oxygen saturation as the inspired gas instantaneously distributes widely throughout the lungs, roughly matching pulmonary blood flow. The lung has a very large diffusion interface (50-75 m^2, about half the size of a tennis court) resulting in a potentially near instantaneous equilibration of alveolar gases with blood. Between pulmonary vein and aorta, there is but the left ventricle as the only opportunity for dispersion, this being slight at normal left ventricular ejection fractions

For this proof-of-concept protocol, we elected to establish a hypoxic baseline, PO_2 < 100 mmHg with increased [dOHb] and reduced BOLD signal. An abrupt change of lung PO_2 to about 100 mmHg would fully saturate the hemoglobin, eliminate dOHb, and raise the BOLD signal.

For over 20 years rapid transitions of lung PCO_2 have been induced by the method of sequential gas delivery [7]. Our aim was to use the same technology to explore and optimize ways of implementing abrupt changes of PO_2 in the lung in order to enable further studies of cerebral hemodynamics such as the measure tissue perfusion using currently available analytical tools including those used for processing dynamic susceptibility contrast perfusion imaging.

Between December 18, 2019 and January 28, 2020 four of the Toronto-based investigators engaged in 5 hourly MRI sessions. Soon thereafter the hospital closed all research studies to focus on COVID-19 related patient care. Despite the small variations in protocols, the authors felt that the generated data was nevertheless remarkably consistent, and had a sufficiently high contrast to noiuse ratio (CNR) to merit an early alert to the imaging community. In this communication, we are able to report: 1) the ability to lower lung PO_2 (and thereby increasing arterial [dOHb] followed by an abrupt rise and fall in lung PO_2 creating a “bolus” of decreasing [dOHb]; 2) the BOLD contrast-to-noise ratio (CNR) resulting from the change in [dOHb]; 3) the degree of [dOHb] bolus dispersion upon arrival in arteries of the brain constituting an effective arterial input function; 4) calculation of standard blood flow parameters.

Methods:

As these methods for inducing [dOHb] changes are totally unprecedented, we were obliged to perform initial exploratory studies to develop the study protocols prior to the IRB application. All subjects were in good health without contraindications to MRI

environment and brief episodes of mild hypoxia, and had given signed consent for the studies.

Respiratory protocol

An investigational computerized gas blender, the RrespirAct™ RA-MR (Thornhill Medical, Toronto, Canada), was used to prospectively target lung PO_2 while maintaining normocapnia independently of ventilation and target lung PO_2 [8,9]. End-tidal PO_2 ($P_{ET}O_2$) was lowered to a baseline of about 55 mmHg (hypoxia baseline) while maintaining normocapnia in order to minimize the changes in arterial PCO_2 (and hence their effect on cerebral blood flow). Hypoxia was maintained for 60 to 90s followed by a gas challenge with the $P_{ET}O_2$ target set to 100 mmHg for 10s to transiently saturate hemoglobin with O_2 before returning to baseline. This normoxic challenge and return to hypoxic baseline was then repeated 3 to 4 times in one session (Figure 1).

Magnetic Resonance Imaging

BOLD images were acquired on a 3T MRI system (Signa HDx - GE Healthcare, Milwaukee) with interleaved echo-planar acquisition during $P_{ET}O_2$ manipulation. The first experiment used a short TR of 200ms, 3 mm isotropic voxels with 3 contiguous slices positioned over the middle cerebral arteries (Figure 1). We identified voxels with large CNR and fit a first order exponential to the rise in BOLD and derived a time constant as a measure of dispersion. A second experiment with 4 normoxic transitions, consisted of 37 contiguous slices with an isotropic resolution of 3mm, field of view of 19.6cm, and TR/TE 2000/30 ms. A high-resolution T1-weighted SPGR sequence was

acquired for co-registering the BOLD images and localizing the arterial and venous components. SPGR parameters included: 176 slices of 1mm thick partitions, in-plane voxel size of 0.85x0.85mm, field of view of 22cm, and TR/TE = 7.88/3.06 msec.

Conversion of end-tidal partial pressure of O_2 ($P_{ET}O_2$) to [dOHb]

The recorded end-tidal $P_{ET}O_2$ was converted to SaO2 using the Hill equation normal sea level physiologic parameters [6]:

$$S_aO_2 = 100\frac{K.(P_{ET}O_2)^n}{1+K.(P_{ET}O_2)^n}$$

Where $n = -4.4921\,.pH + 36.365$; $K = 5.10^{-142}.pH^{157.31}$; *pH = 7.4*

[dOHb] = [Hb] x (1-SaO_2)

Image Analysis

All image analysis was performed using Matlab 2015a and AFNI [10]**.** The 3-slice dataset with a short TR of 200ms was visually inspected and one voxel with high CNR localized over the middle cerebral artery was chosen to analyze the rise-time (τ) of the BOLD signal. τ is the time constant of the exponential function fitted to the BOLD signal. The pre-processing steps for the whole brain dataset with TR of 2000ms included slice time correction, volume re-registration, and fourth degree polynomial detrending. SaO2 was resampled to TR intervals and time-aligned to the whole brain average BOLD signal. The baseline BOLD signal (S_0) was then defined as the mean of the BOLD signal (S_t) over five time-frames including the duration of the baseline before the first bolus, 10 sec

before the second, third and fourth boluses, and 10 sec before the end of the protocol. The scaled BOLD signal ($S_{c,t}$) could then be calculated as $\frac{S_t - S_0}{S_0}$.

ΔBOLD, CNR and TD

A time delay (TD) map was calculated using cross-correlation between $S_{c,t}$ and multiple $S_a O_2$ curves time shifted from 0 to 5 sec by intervals of 0.1 s. The time shift needed to obtain maximum correlation (R) with $S_{c,t}$ was extracted for each voxel to generate a time delay.

$S_{c,t}$ was regressed against the voxel-wise shifted $S_a O_{2,t}^{shifted}$ to calculate the slope of regression:

$$S_{c,t} = \alpha . S_a O_{2,t}^{shifted} + \varepsilon_t$$

with α = slope of the regression and ε_t the residuals.

Using the slope of the regression α, BOLD signal change (ΔBOLD) and CNR were computed as:

$$\Delta\text{BOLD} = \alpha . (max(S_a O_{2,t}^{shifted}) - min(S_a O_{2,t}^{shifted}))$$

$$CNR = \frac{\Delta BOLD}{std(\varepsilon_t)}$$

In order to examine whether signal averaging would improve bolus definition, CNR was calculated for 1, 2, 3 and finally all 4 gas challenges: the range of each segment was defined as 0-190 sec, 0-290 sec, 0-390 sec, 0-490 sec.

Tracking of contrast in arteries and veins

Arterial and venous voxels were extracted using $\Delta BOLD$, R, and TD. Arterial voxels were defined as all voxels with $\Delta BOLD > 20\%$, R > 0.8 and 0 < TD < 1.5 sec. Venous voxels were defined as all voxels with $\Delta BOLD > 20\%$, R > 0.8 and 3 < TD < 5. BOLD time series was averaged within the arterial and venous components over the four boluses. The SaO_2 was also averaged over the four boluses. The averaged arterial and venous components were plotted along with SaO_2 (Figure 2c).

Cerebral blood volume (CBV)

Quantitative CBV was calculated as follow:

CBV [mL/g] = $\left(\frac{k_H}{\rho}\right) . \left(\frac{AUC}{AUCv}\right)$

Tissue density: ρ = 1.04 g/cc

Difference in hematocrit in large vessels

and capillaries: k_H = 0.73

k_H/ρ = 0.705 cc/g

AUC is the area under the curve of the BOLD signal (S_t) over the entire protocol. AUCv is the area under the curve for a voxel containing blood only with large AUC. We set this value to corresponds to the 5 percentile of the largest AUC.

Mean transit time (MTT) and cerebral blood flow (CBF)

Standard tracer kinetic modeling was used to calculate MTT and CBF as per:

$S_t = AIF_t \otimes (CBF \times R_t)$

Subscript t indicates that the variable is a function of time.

S_aO_2 was used as the arterial input function (AIF_t) and was scaled to have an AUC equal AUCv.

$R_t = e^{-t/MTT}$ was used for the residue function. It is equal to 1 at time 0 and set to 0 at time equal to 5 x MTT. CBF and MTT can then be determined using least square fitting procedure. MTT was bound between 0 and 7s.

Gray and white matter measurements

The T1-weighted images were segmented into gray matter, white matter and cerebrospinal fluid using spm8 software package [11]. The probability density maps obtained were thresholded at 0.8 to generate a mask for gray matter (GM) and white matter (WM). One layer of peripheral voxels was eroded from the white matter mask to minimize partial volume effects.

Gray and white matter mask were used to calculate average values of BOLD signal, CNR, TD, MTT, CBV and CBF. A paired t-test was also computed to assess the change in CNR for each set of merged boluses.

Results:

Figure 1 illustrates the extent of dispersion inclusive of that in the lung, confluence in the pulmonary vein, wash-in and wash-out of the left ventricle, and any mixing in the aorta and extracranial arteries. The small extent of observed dispersion indicates rapid changes of [dOHb] in the lungs and little dispersion in the heart. There is also remarkable consistency in the successive gas challenges and resulting BOLD changes with little drift (Figure 1 b). Figure 2b illustrates that the distribution of early arriving

large amplitude voxels (red) are consistent with the locations of middle cerebral arteries, and the later arriving large amplitude changes, colored blue, are consistent with the location of the major veins and venous sinuses. The CNR was sufficiently large that averaging results of gas challenges resulted in minimal improvement of CNR. CNR in gray matter was 3.28±2.07, 3.35±2.11, 3.61±2.26 and 3.73±2.29 respectively for 1, 2, 3 and 4 oxygen challenges. In white matter CNR was 1.93±1.03, 1.97±1.02, 2.19±1.11 and 2.25±1.13. Although changes in CNR for each additional bolus are not large, a Bonferroni corrected paired t-test showed that all of the changes were significant ($p < 0.001$) for both gray and white matter.

Figure 2a shows BOLD signal change clearly distinguished large vessels, gray matter, and white matter. The average gray matter ΔBOLD was 7.42±9.13% and the average white matter ΔBOLD was 2.66±1.94%. In figure 2b, the calculated time delay metric effectively distinguishes large arteries (TD < 1.5s) including the middle cerebral artery and the sinovenous structures (TD > 3s) including the sagittal, straight, and transverse sinuses. From the time delay map, an average TD of 1.84±1.18s in gray matter and 3.37±1.53s in white matter was calculated (Figure 3). Figure 2c shows the average BOLD signal over arterial and venous voxels separately. This average was calculated over the four gas challenges. Delay maps show close matching to tissue types (Figure 3). Maps displaying CBV, MTT and CBF calculated from the generated data are shown in Figure 4. Average CBV, MTT and CBF were calculated within gray and white matter masks, as well as their ratio. Venous voxels as defined earlier were removed from the gray matter mask. Values of perfusion metrics are listed in table 1 (under dHb bolus) showing good agreement with published literature values.

Table 1

	Gray matter			White matter		
Source	CBV (ml/100g)	CBF (ml/100g/min)	MTT (sec)	CBV (ml/100g)	CBF (ml/100g/min)	MTT (sec)
dHb bolus	3.7	69.9	3.9	2.6	19.4	7.1
Frackowiak et al[12]	N/A	65.3±11	N/A	N/A	21.4±9.0	N/A
Lenzi et al[13]	N/A	64.5±17.3	N/A	N/A	21.16±2.74	N/A
Ito et al[14]	3.8±0.7	44.4±6.5	N/A	N/A	N/A	N/A
Heijtel et al[15]	3.21±0.45	46.3±7.0	N/A	1.87±0.31	30.2±3.9	N/A
Watabe et al[16]	N/A	N/A	N/A	1.78±0.22	21.3±2.7	N/A

Figure 1

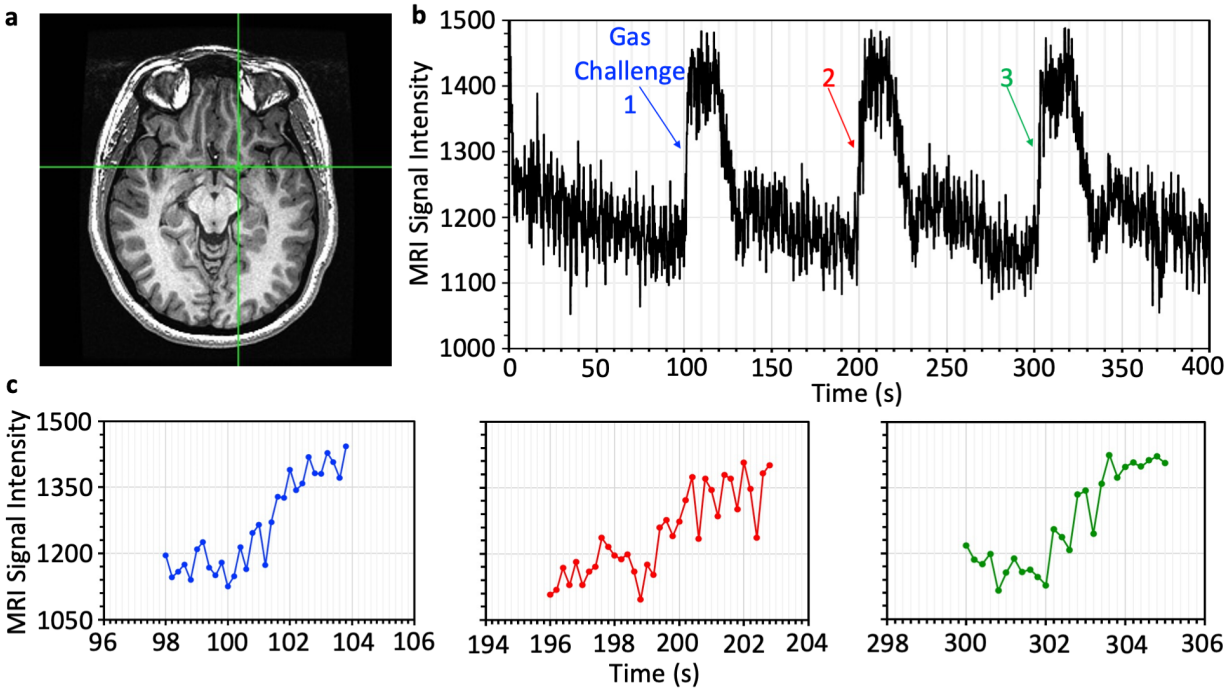

Figure 1: Gas challenge and BOLD arterial signal*. The protocol was first carried out with a short TR = 200 ms for measuring response time. A voxel overlying the middle*

cerebral artery (green cross–hairs) with a large change in BOLD signal was chosen to represent the arterial signal rise time. The first 3 normoxic challenges are shown. ***a****: Location of the voxel.* ***b****: BOLD signal vs. time for 3 consecutive challenges.* ***c****: Expanded time scale of the BOLD signal change in B from baseline to normoxia. Fitting a first order exponential to the rise in the BOLD signal results in time constants of 1.21 s, 1.67 s and 2.10 s respectively.*

Figure 2

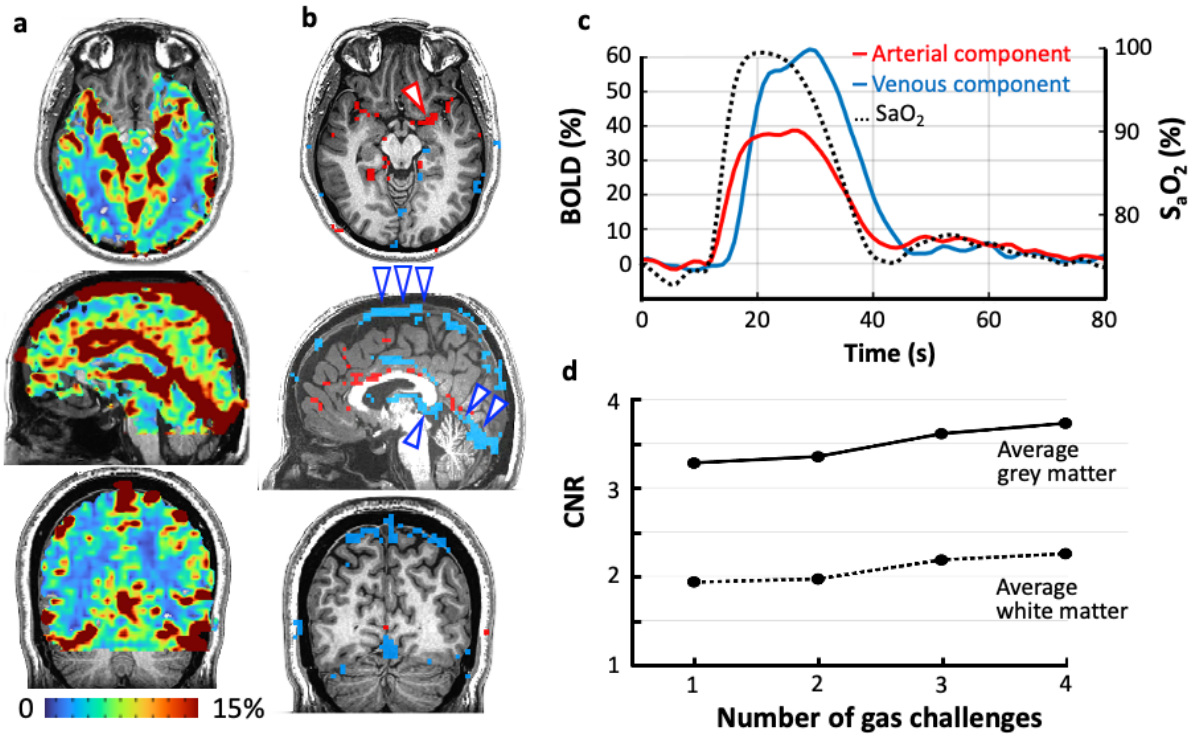

Figure 2: Changes in BOLD signal due to changes in deoxyhemoglobin concentration [dOHb].

The protocol was carried out with TR = 2000 ms. ***a:*** *Maps of BOLD signal change (Δ BOLD).* ***b:*** *Large arteries and veins can be distinguished based on arrival time differences (see C) and amplitude of the paramagnetic bolus. Criteria for identifying*

arterial voxels were: Δ BOLD > 20%, R > 0.8, TD < 1.5 sec with R = correlation value between oxygen saturation (SaO_2) and BOLD signal (TD = arrival time delay). For venous voxels criteria were: Δ BOLD > 20%, R > 0.8, TD > 3 sec. Criteria for arterial voxels highlighted the middle cerebral artery (red wedge). Identification of large veins is confirmed on visual inspection of the maps as voxels that contain the highest volume of blood and least volume averaging with adjacent low blood volume tissues will have the largest signal change. Late filling voxels co-localized with known large sinovenous structures: superior sagittal sinus (3 blue wedges), straight sinus (2 blue wedges), and Great vein of Galen (one blue wedge). ***c:*** *Graph showing bolus arrival times. The SaO_2 curve was calculated from $P_{ET}O_2$ data synchronized with the rise in arterial BOLD signal. The rise in the arterial signal precedes the rise in the venous signal as expected. The larger magnitude of the venous BOLD signal was attributed to lower baseline of unscaled BOLD signal as well as larger vein caliber.* ***d:*** *The contrast to noise ratio (CNR) for 1 gas challenge, as well as the CNR after averaging over 2, 3 and 4 gas challenges for gray matter and white matter. Averaging over successive challenges does not add substantially to CNR.*

Figure 3

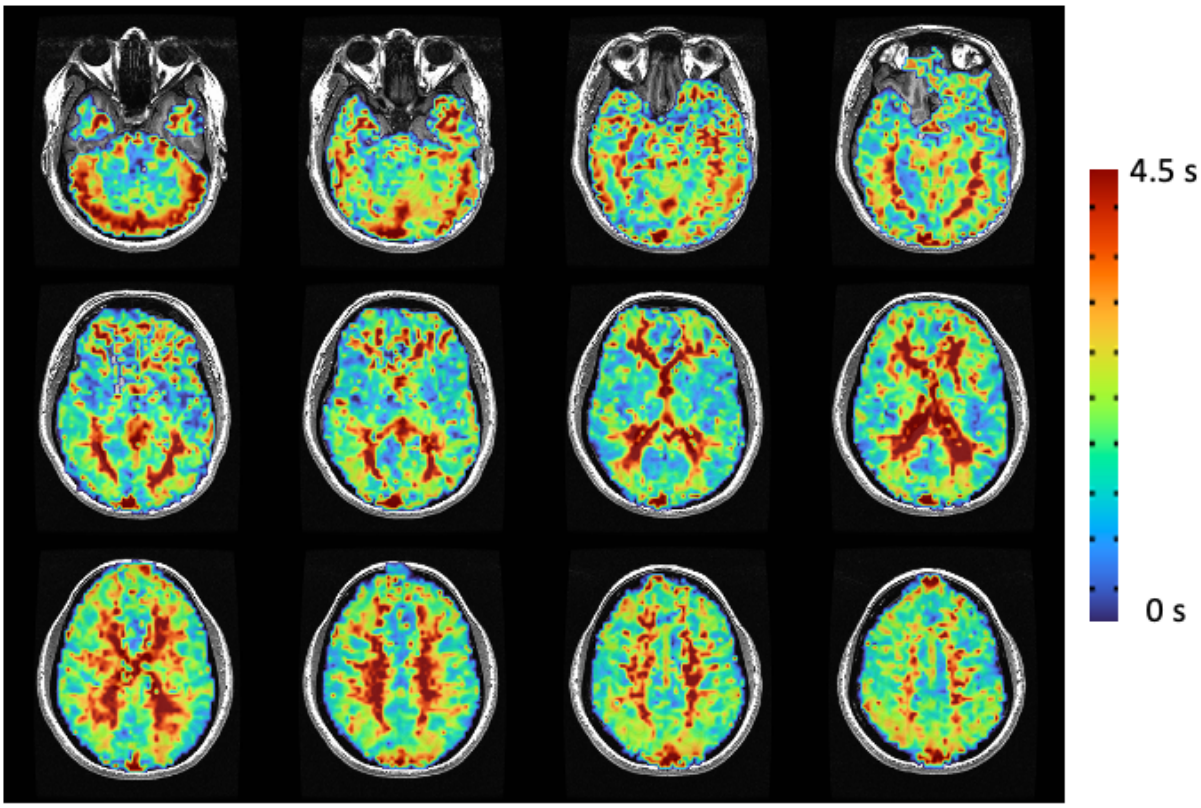

Figure 3: Time Delay (TD) map

The map shows sharp delineation between initial arrival of the oxyhemoglobin bolus in gray matter (blue/green), followed by subcortical and deep white matter (green/yellow), and late arrival in periventricular white matter and veins (orange/red) consistent with the known cerebral vascular kinetics.

Figure 4

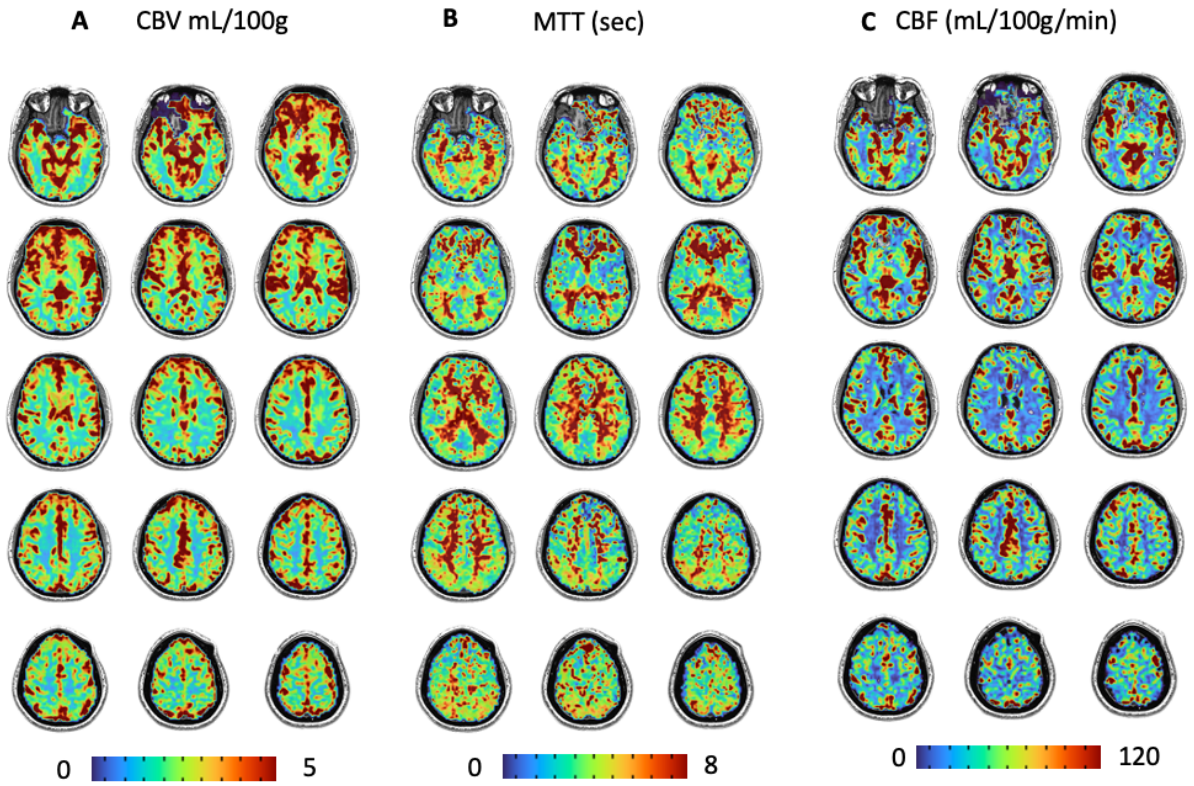

Figure 4: Perfusion metrics

Cerebral blood volume (CBV); (mean transit time (MTT);, cerebral blood flow (CBF).

Discussion:

We report important incidental findings in the course of protocol development prior to IRB application which are akin to a medical case report. Furthermore, the subjects were the investigators themselves and thus were well informed and had all signed consent forms. As we were examining protocols, our protocols were not consistent across the 5 subjects. Nevertheless, the consistency and CNR of the data provides sufficient confidence to report our findings. We will commence properly constituted

follow-up studies when facilities re-open for research, but we feel these early reports will enable earlier reproduction and follow-up by others in the wider imaging community.

The main findings from this preliminary study are that steady baseline levels of hypoxia and hemoglobin desaturation can be maintained (Supplemental Figure 1), and that ventilatory challenges can effect an abrupt decrease in [dOHb] in the course of 10s, followed by a rapid return to the baseline saturation (Figure 1). This rapid reduction in [dOHb] is reflected in a rapid increase in BOLD signal with high CNR throughout the arterial and venous compartments of the brain (Figure 2d). The rapidity of the change in BOLD implies a rapid change in [dOHb] in the lung and little dispersion of the bolus prior to arrival in the brain vasculature. The degree of dispersion observed would compare favorably to that of intravenously injected contrast agents as it eliminates an entire pathway over which dispersion can develop including, the brachial vein, the subclavian vein, the right atrium, and the right ventricle. Rapid contrast generation in the lung bypasses this segment of the dispersive pathway, with subsequent dispersion only occurring due to passage within the left atrium and left ventricle with the latter dispersion depending on the left ventricular ejection fraction. The respiratory source of contrast generation therefore enables an arterial contrast bolus as close to a square wave input function as possible short of direct of contrast injection into large arteries.

As expected, the rise in the arterial signal precedes the rise in the venous signal. The larger magnitude of the venous BOLD signal is likely due to a lower baseline of the unscaled BOLD signal. When scaling, dividing by a lower baseline will yield a higher

percent change BOLD signal. Venous voxels are indeed expected to have a lower raw BOLD signal baseline because of higher [dOHb]. An additional reason for this difference in magnitude is attributed to smaller partial voluming artifact in veins where the caliber is larger than in arteries.

Induction of hyperoxia has also been used to induce BOLD signal changes to enable the measure of CBF, CBV and MTT[17] The signal characteristics with hyperoxia differ from intravascular bolus contrast or from abrupt inhalations as in our method.

The hyperoxic inhalation does not change the [dOHb] in the arteries. On arrival to the tissues, the oxygen dissolved in the plasma is used by the tissues for metabolism, sparing oxygen bound to hemoglobin. Thus there is no arterial input function (AIF) but the reduction in [dOHb] at the tissues, increases the BOLD signal. Our method changes the [dOHb] in the arterial blood thereby inducing a measurable AIF. As the oxygen content of the blood changes, the effects are of course passed on to the tissues and the BOLD signal reflects the net [dOHb]. Whereas *hyper*oxia results in hyperventilation, reductions in PCO_2 and thus cerebral blood flow[18], cerebral blood flow remains constant at the range of 100 mmHg to 45 mmHg[19]

Finally, in terms of safety to exposure to brief periods of hypoxia, there is no evidence that it is harmful. Pathological exposures to hypoxia such as those caused by pneumonia, is associated with regional lung collapse. Otherwise, hypoxia is well tolerated. For example, in La Paz, the capital city of Bolivia at 4000 m elevation, most of the population, as well as visitors have PO_2 in the range of 50-60 mmHg, which may be associated with some limitation in exercise tolerance, but not illness. A popular past-

time for the tourists is to climb to 6000 m and beyond. These climbs and their exacerbation of hypoxia are not known to result in myocardial infarctions or strokes or other hypoxic injury. Similar tolerance of severe hypoxia is observed in visitors to other highlands in South America, Europe, Himalayas, China, Asia and Africa (Ethiopia). To provide further perspective, most of the human population undergoes multiple episodes of apnea (breath-holding) during sleep. Depending on body habitus, underlying lung and heart diseases, PO_2 frequently has been observed to fall to values 30-40 mmHg[6]. Thus the PO_2 of 50-55 mmHg is well tolerated by humans and frequently encountered as part of day-to-day living. In our study, the level of PO_2 was virtually imperceptible, causing no distress to any of the 5 subjects.

In this study, hypoxia was established as a baseline and a normoxic bolus with increasing oxyhemoglobin concentration used as the stimulus. The same imaging principles would apply in the reverse situation with a normoxic baseline and hypoxic gas challenges with increasing deoxyhemoglobin concentration. This latter approach would reduce safety concerns in some patients with co-morbidities. The hypoxic baseline was chosen in these studies because the conditions for rapid transition to normoxia were more readily attained at the time of the study than the reverse. Implementation of the study using normoxia as the baseline is planned in continuing studies.

We conclude that the use of [dOHb] changes as a non-invasive intra-vascular MRI contrast agent is feasible.

Acknowlegment

The authors would like to thank Dr. Adrian Crawley for his immeasurable support, insightful advice and constructive critique that has contributed towards this research work. We would also like to thank our RespirAct™ engineer, Vepeson Wijeya for his technical support to ensure the experiments were carried out uninterrupted, our valued research coordinator Aberami Skandaraniyam as well as the Toronto Western Hospital MRI technologists, Keith Ta and Asma Naheed, for their patience as we refined our experimental protocol. The study was supported by the Andreae Vascular Dementia Research Unit in the Joint Department of Medical Imaging at The University Health Network and a research grant to Dr. Kamil Uludag from the Institute for Basic Science, Suwon, Republic of Korea (IBS-R015-D1).

Authors Contributions

All listed authors contributed to the work; no authors who contributed to the work are excluded from the author list. All authors are aware of, and agree with the data. Authors agree to the Journal's copyright policy and agree to cover all costs should it be accepted for publication.

Disclosures

Drs Fisher and Mikulis contributed to the development of an automated end-tidal targeting device, RespirAct™ which is designed, assembled, and made available as a research tool by Thornhill Medical Inc (TMI). TMI is a for profit spin-off company from the University Health Network/University of Toronto. Drs Fisher and Mikulis have equity in TMI. J. Poublanc, O. Sobczyk, R. Shafi, J. Duffin, K. Uludag, J. Wood, C. Vu, R. Dharmakumar declare no competing interests.

References

1. Ogawa, S., Lee, T. M., Kay, A. R. & Tank, D. W. Brain magnetic resonance imaging with contrast dependent on blood oxygenation. *Proc. Natl. Acad. Sci. U. S. A.* (1990). doi:10.1073/pnas.87.24.9868

2. Zhao, J. M., Clingman, C. S., Närväinen, M. J., Kauppinen, R. A. & Van Zijl, P. C. M. Oxygenation and hematocrit dependence of transverse relaxation rates of blood at 3T. *Magn. Reson. Med.* (2007). doi:10.1002/mrm.21342

3. Spees, W. M., Yablonskiy, D. A., Oswood, M. C. & Ackerman, J. J. H. Water proton MR properties of human blood at 1.5 Tesla: Magnetic susceptibility, T1, T2*, T2, and non-Lorentzian signal behavior. *Magn. Reson. Med.* (2001). doi:10.1002/mrm.1072

4. Uludağ, K., Müller-Bierl, B. & Uğurbil, K. An integrative model for neuronal activity-induced signal changes for gradient and spin echo functional imaging. *Neuroimage* (2009). doi:10.1016/j.neuroimage.2009.05.051

5. Boxerman, J. L. *et al.* The intravascular contribution to fmri signal change: monte carlo modeling and diffusion-weighted studies in vivo. *Magn. Reson. Med.* (1995). doi:10.1002/mrm.1910340103

6. Balaban, D. Y. *et al.* The in-vivo oxyhaemoglobin dissociation curve at sea level and high altitude. *Respir. Physiol. Neurobiol.* **186**, 45–52 (2013).

7. Fierstra, J. *et al.* Measuring cerebrovascular reactivity: What stimulus to use? *Journal of Physiology* (2013). doi:10.1113/jphysiol.2013.259150

8. Slessarev, M. *et al.* Prospective targeting and control of end-tidal CO2 and O2

concentrations. *J. Physiol.* (2007). doi:10.1113/jphysiol.2007.129395

9. Ito, S. *et al.* Non-invasive prospective targeting of arterial PCO2 in subjects at rest. *J. Physiol.* (2008). doi:10.1113/jphysiol.2008.154716

10. Cox, R. W. AFNI: Software for analysis and visualization of functional magnetic resonance neuroimages. *Comput. Biomed. Res.* (1996). doi:10.1006/cbmr.1996.0014

11. Ashburner, J. & Friston, K. J. Unified segmentation. *Neuroimage* (2005). doi:10.1016/j.neuroimage.2005.02.018

12. Frackowiak, R. S. J., Lenzi, G. L., Jones, T. & Heather, J. D. Quantitative measurement of regional cerebral blood flow and oxygen metabolism in man using15O and positron emission tomography: Theory, procedure, and normal values. *J. Comput. Assist. Tomogr.* (1980). doi:10.1097/00004728-198012000-00001

13. Lenzi, G. L., Frackowiak, R. S. J. & Jones, T. CMRO2 and CBF by the oxygen-15 inhalation technique. results in normal volunteers and cerebrovascular patients. *Eur. Neurol.* **20**, 285–290 (1981).

14. Ito, H. *et al.* Database of normal human cerebral blood flow, cerebral blood volume, cerebral oxygen extraction fraction and cerebral metabolic rate of oxygen measured by positron emission tomography with 15O-labelled carbon dioxide or water, carbon monoxide and oxygen: A multicentre study in Japan. *Eur. J. Nucl. Med. Mol. Imaging* **31**, 635–643 (2004).

15. Heijtel, D. F. R. *et al.* Quantitative agreement between [15O]H2O PET and model free QUASAR MRI-derived cerebral blood flow and arterial blood volume. *NMR Biomed.* **29**, 519–526 (2016).

16. Watabe, T. *et al.* CBF/CBV maps in normal volunteers studied with 15O PET: a possible index of cerebral perfusion pressure. *Neurosci. Bull.* **30**, 857–862 (2014).

17. MacDonald, M. E., Berman, A. J. L., Mazerolle, E. L., Williams, R. J. & Pike, G. B. Modeling hyperoxia-induced BOLD signal dynamics to estimate cerebral blood flow, volume and mean transit time. *Neuroimage* (2018). doi:10.1016/j.neuroimage.2018.05.066

18. Iscoe, S., Beasley, R. & Fisher, J. A. Supplementary oxygen for nonhypoxemic patients: O2 much of a good thing? *Crit. Care* (2011). doi:10.1186/cc10229

19. Mardimae, A. *et al.* The interaction of carbon dioxide and hypoxia in the control of cerebral blood flow. *Pflugers Arch. Eur. J. Physiol.* (2012). doi:10.1007/s00424-012-1148-1